Low-intensity, Long-wavelength Red Light Slows the Progression of Myopia in Children: an Eastern China-based Cohort

Lei Zhou
   Ningbo Eye Hospital

Chao Xing
   the Second Affiliated Hospital of Wenzhou Medical University

Wei Qiang
   Ningbo Eye Hospital

Chaoqun Hua
   Ningbo Eye Hospital

Liyang Tong (✉ liyang_tong20@126.com)
   Ningbo Eye Hospital

Abstract

Myopia is prevalent worldwide, particularly in East and Southeast Asia. Recent studies have suggested that the spectral composition of ambient lighting influences refractive development, especially in humans. We aimed to determine the effect of 650-nm single-wavelength red light on the inhibition of myopia progression in children. In this retrospective cohort study, 105 myopic children (spherical equivalent refractive error [SER], -6.75 to -1.00 dioptres (D)) aged from 4 to 14 years old were retrospectively reviewed. Subjects were treated with 650-nm, low-intensity, single-wavelength red light twice a day for 3 minutes each session, with at least a 4-hour interval between sessions. IOL Master was utilized to measure the axial length (AL) and corneal curvature. Choroidal images were assessed using enhanced depth imaging optical coherence tomography (EDI-OCT), and the luminal area (LA) and stromal area were converted to binary images by the Niblack method. At baseline, the mean SER was -3.09 ± 1.74 D and -2.87 ± 1.89 D at 9 months, and significant changes occurred over time (P = 0.019). The AL increased by -0.06 ± 0.19 mm for 9 months (0.21 ± 0.15 mm pretreatment; P⬛0.001). The subfoveal choroidal thickness (SFChT) had changed by 45.32 ± 30.88 μm at the 9-month examination (P⬛0.001). Repetitive exposure to 650-nm, low-intensity, single-wavelength red light effectively slowed the progression of myopia and reduced axial growth after short treatment durations. These results require further validation in a longitudinal study, as well as further research in animal models.

Introduction

Myopia, a refractive condition associated with visual impairment and vision loss, is the most common eye disorder worldwide.[1−3] In recent decades, the prevalence of myopia in children and adolescents has been dramatically increasing; the onset age has decreased, while the severity of myopia has rapidly increased.[4,5] It is estimated that by 2050, 49.8% of the global population will have myopia, and 9.8% will have high myopia.[1] During the coronavirus disease 2019 (COVID-19) pandemic, the myopia rate in primary and middle school students increased by 11.7% in six months in China. In particular, the results of a survey released by the Chinese Ministry of Education at the end of August 2020 highlighted the problem of myopia.

Currently, there is no effective intervention to prevent the progression of myopia. Young adults can wear orthokeratology (OK) contact lenses or take the muscarinic antagonist atropine in hospital-based interventions, which have had only limited success, although low-dose atropine eyedrops have shown promise.[6−9] The long-term use of atropine is associated with side effects such as photophobia, rebound myopia and drug resistance. In this context, exploring new methods to prevent and control myopia in young people has become a top priority. Thus, we focused on low-intensity, long-wavelength red light therapy as a new method to help restrict the progression of myopia by stimulating longer-wavelength-sensitive (LWS) cones,[10] improving mitochondrial complex activity,[11] producing slower axial elongation and preventing the normal decrease in refraction.[12−16]

Recent studies have suggested that spending time outdoors may prevent the development of myopia.[17,18] The protective association appears to be related to the higher ambient illuminances and the spectral composition of ambient light rather than engaging in sport activities, because the time spent engaged in an indoor sport activity is not associated with a lower likelihood of myopia.[17] Because both luminance and chromatic signals can influence emmetropization, alterations in the spectral composition of ambient lighting could influence refractive development in different ways.[13] The spectral composition of indoor lighting produced by tungsten or light-emitting diodes (LEDs) is different from that of sunlight, which may play a role in the inhibitory effect on myopia.[19] Some previous studies suggested that reducing potential chromatic cues associated with longitudinal chromatic aberration (LCA) by restricting the spectral composition of ambient light interferes with emmetropization and supports the hypothesis that chromatic cues may normally contribute to the regulation of refractive development.[13]

The effects of the spectral composition of light on refractive development have been studied in a number of animal models.[10,12,14,19–24] It is important to determine how and the extent to which the wavelength composition of ambient lighting influences refractive development, especially in humans, because it may be possible to manipulate the spectral characteristics of ambient lighting in ways that could have a therapeutic benefit.

The purpose of this study was to assess the efficacy of 650-nm, low-intensity, single-wavelength red light therapy for preventing the progression of myopia and inhibiting the excessive elongation of axial length (AL) in school children, similar to ambient outdoor sunlight.

Results

A total of 105 children (49 girls and 56 boys) with a mean age of 8.97 ± 2.36 years whose myopia progression and axial elongation were accelerated were enrolled in the study. The mean SER was − 3.09 ± 1.74 D at baseline and was − 3.02 ± 1.65, -2.90 ± 1.44 and − 2.87 ± 1.89 D at 3 months, 6 months, and 9 months, respectively. The mean corneal curvature was 42.89 ± 1.90, 42.90 ± 1.91, 42.94 ± 1.81 and 42.86 ± 1.96 D at baseline and at the various timepoints up to the 9-month follow-up, respectively, with no significant differences (P = 0.174). During the same period, the mean AL slightly decreased over time from 24.81 ± 1.31 mm to 24.74 ± 1.29, 24.72 ± 1.34 and 24.75 ± 1.30 mm after repeated red-light irradiation, and the changes were statistically significant (Table 1 and Table 2). Briefly, there was a steady increase in the SER and AL before red light therapy, while the opposite trend was observed after treatment (Fig. 1). The corneal curvature slightly increased at first and then slightly decreased, but there was no significant difference.

Table 1

Demographic and Biometric Characteristics of all the Participants at Different Time Points (n = 105; 49 girls, 56 boys, mean ± SD)

Characteristics	Range	Baseline	Three months	Six months	Nine months
Age	4 to 14	8.97 ± 2.36			
SER (D)	-6.75 to -1.00	-3.09 ± 1.74	-3.02 ± 1.65	-2.90 ± 1.44	-2.87 ± 1.89
CC (D)	39.2 to 46.11	42.89 ± 1.90	42.90 ± 1.91	42.94 ± 1.81	42.86 ± 1.96
AL (mm)	22.50 to 27.3	24.81 ± 1.31	24.74 ± 1.29	24.72 ± 1.34	24.75 ± 1.30
SER: spherical equivalent refractive error; CC: corneal curvature; AL: axial length.					

Table 2 displays the changes in biometric characteristics of all the participants in different subgroups at different time points. For the school-age children (8–14 years old), the SER changed by -0.19 ± 0.08, 0.14 ± 0.10, 0.29 ± 0.16 and 0.31 ± 0.24 D (P = 0.027) at baseline, 3 months, 6 months, and 9 months, respectively. The changes in school-age children were slightly greater than those of preschool children (4–7 years old) (-0.30 ± 0.15, 0.06 ± 0.11, 0.13 ± 0.10 and 0.20 ± 0.14 D, P = 0.034), and the difference was significant (P = 0.021). Correspondingly, for the 8–14 years old group, the increases in the AL were 0.21 ± 0.13, -0.08 ± 0.11, -0.10 ± 0.15 and − 0.06 ± 0.18 mm (P < 0.001) at baseline, 3 months, 6 months, and 9 months, respectively, which were slightly greater than those in the preschool subjects (4–7 years old) (0.22 ± 0.18, -0.06 ± 0.12, -0.06 ± 0.19 and − 0.02 ± 0.22 mm, P < 0.001), and the differences were significant (P = 0.05). The corneal curvature decreased by -0.00 ± 0.51, -0.02 ± 0.34, -0.03 ± 0.46 and − 0.14 ± 0.60 D at each sampling point, but the changes were not statistically significant (P = 0.174). The disparity between the four subgroups was also not statistically significant (for the age groups, P = 0.832; for the AL groups, P = 0.494).

Table 2

Change in Biometric Characteristics of all the Participants at Different Time Points (n = 105; 49 girls, 56 boys, mean ± SD)

Characteristics			For age（years）		For AL (mm)	
		Total	4-7 years （n=29）	8-14 years (n=76）	≤24mm （n=25）	＞24mm （n=80）
Change in SER (D)	Baseline	-0.27±0.11	-0.30±0.15	-0.19±0.08	-0.20±0.14	-0.26±0.17
	3 months	0.07±0.14	0.06±0.11	0.14±0.10	0.05±0.09	0.13±0.14
	6 months	0.19±0.25	0.13±0.10	0.29±0.16	0.07±0.14	0.39±0.19
	9 months	0.22±0.17	0.20±0.14	0.31±0.24	0.16±0.20	0.42±0.30
P value		0.019[a]	0.034[a]	0.027[a]	0.022[a]	0.006[a]
			F=4.562, *P*=0.021[b]		F=6.708, *P*<0.001[b]	
Change in CC (D)	Baseline	-0.00±0.51	0.01±0.17	-0.00±0.58	0.04±0.50	-0.13±0.51
	3 months	-0.02±0.34	-0.02±0.16	-0.02±0.39	-0.02±0.36	-0.00±0.29
	6 months	-0.03±0.46	0.01±0.21	-0.05±0.53	-0.03±0.44	-0.03±0.49
	9 months	-0.14±0.60	-0.23±0.68	-0.09±0.53	-0.04±0.41	-0.32±0.80
P value		0.174[a]	0.016[a]	0.771[a]	0.075[a]	0.548[a]
			F=0.045, *P*=0.832[b]		F=0.468, *P*=0.494[b]	
Change in AL (mm)	Baseline	0.21±0.15	0.22±0.18	0.21±0.13	0.20±0.16	0.22±0.14
	3 months	-0.07±0.19	-0.06±0.12	-0.08±0.11	-0.03±0.09	-0.09±0.12
	6 months	-0.09±0.11	-0.06±0.19	-0.10±0.15	-0.03±0.23	-0.11±0.16
	9 months	-0.06±0.19	-0.02±0.22	-0.06±0.18	-0.04±0.18	-0.08±0.19
P value		<0.001[a]	<0.001[a]	<0.001[a]	<0.001[a]	<0.001[a]
			F=3.839, *P*=0.050[b]		F=29.486, *P*<0.001[b]	

The mean SFChT was 223.38 ± 69.81 mm at baseline and significantly increased to 268.71 ± 73.59 mm at 9 months after repeated narrow-band, long-wavelength light irradiation ($P < 0.001$). The baseline TCA was 0.43 ± 0.12 mm^2; the LA was 0.28 ± 0.08 mm^2 and the stromal area was 0.15 ± 0.04 mm^2, which yielded a mean CVI of 0.65 ± 0.02. Nine months after the treatment, both the TCA (0.48 ± 0.13 mm^2) and the LA (0.33 ± 0.09 mm^2) were significantly higher than those at baseline (both $P < 0.001$, Table 3). The stromal area (0.14 ± 0.04 mm^2) was significantly lower than the baseline stromal area ($P < 0.001$, Table 3). The CVI was 0.69 ± 0.04 at 9 months after the treatment, which was not significantly different from the baseline CVI ($P = 0.433$).

Table 3
Choroidal Characteristics of all the Participants in the Choroidal Binarization Method (n = 105; 49 girls, 56 boys, mean ± SD)

Characteristics	Baseline	Nine months	P
SFCHT (μm)	223.38 ± 69.81	268.71 ± 73.59	< 0.001*
Total choroidal area (mm^2)	0.43 ± 0.12	0.48 ± 0.13	< 0.001*
LA (mm^2)	0.28 ± 0.08	0.33 ± 0.09	< 0.001*
Stromal area (mm^2)	0.15 ± 0.04	0.14 ± 0.04	< 0.001*
Choroidal vascularity index (LA/TCA)	0.65 ± 0.02	0.69 ± 0.04	0.433†

SFChT: subfoveal choroidal thickness; LA, luminal area; TCA, total choroidal area. * P value determined by paired t–test. † P value determined by Wilcoxon signed–rank test.

To understand the relationship between changes in parameters and baseline factors, Pearson's correlation coefficient was used. A scatter plot graph of the change in the AL at 9 months and age is shown in Fig. 3(A). At the 9-month visit, the change in the AL was found to be significantly associated with age at enrolment (R = -0.229, $P = 0.002$). We also found a significant correlation between the change in AL and baseline AL in the study (R = -0.34, $P < 0.001$) (Fig. 3(B)). According to univariate linear regression analysis, the decrease in AL had a positive relationship with age at enrolment and baseline AL; the decrease in AL was larger in individuals who were older and who had a longer baseline AL.

Discussion

It is well established that spending time outdoors may prevent the development of myopia, although the underlying mechanism is unknown.[6,17,18,29] The dominant theory is that exposure to brighter sunlight

outside stimulates a release of dopamine in the retina, and dopamine can promote slower, normal growth of the eye, thereby leading to a lower risk of myopia.[30]

Recently, some novel findings have supported that the differences in the spectral composition of lighting in indoor and outdoor environments may contribute to the higher prevalence of myopia in children who spend less time outdoors.[13] The chromaticity signals from LCA can promote the normal rate of eye growth and development of ocular refraction,[31] which may help to explain why outdoor activity has a protective effect against myopia and to highlight the possible effects of artificial light in the increasing prevalence of childhood myopia. Therefore, the manipulation of the chromaticity of light to which the eyes are exposed may be valuable for the management or prevention of childhood myopia. To date, we know relatively little about how variations in the wavelength composition of ambient lighting affect refractive development in humans. Our goal was to determine whether environments dominated by long-wavelength red light inhibit the development of myopia. The study programme integrated red light with a wavelength of 650 nm in natural light, which is beneficial to the human body, to replace natural light, irradiate the retina with safe power and effective time, and stimulate the retina to produce and release more dopamine, thereby effectively controlling axial eye growth and preventing the occurrence and progression of myopia.

In the present study, children who received repeated 650-nm red light irradiation developed relative hyperopic refractions, and significant changes occurred over time (P = 0.019, Table 2). Corresponding to refractive development, the treated eyes of all children exhibited statistically significantly slower axial eye growth than before treatment. Our results showed that low-intensity, single-wavelength red light irradiation can effectively control AL elongation and slow myopia progression (Table 2, Fig. 2). Interestingly, the decreases in both the SER and AL in the older group (8–14 years) were greater than those in the younger group (4–7 years), which is consistent with previous studies. The decreases in the SER and AL in the longer AL group (≥ 24 mm) were greater than those in the shorter group (< 24 mm). Notably, no significant differences in corneal curvature were found pretreatment and posttreatment. These results suggest that the slowed myopia progression was mainly due to AL shortening and not corneal curvature flattening. Regardless of the exact mechanism that was responsible for the hyperopic shifts found in the present study, the results suggest that exposure to long-wavelength lighting may, at least under certain circumstances, be beneficial for reducing myopia progression. The results also support the emerging view that the eye can utilize chromatic cues associated with LCA to regulate ocular growth.[13,31]

Whether certain spectral ranges of light can more potently delay and inhibit myopia than others is a topic of ongoing research. The effects of the spectral composition of light on refractive development have been studied in a number of animal models. When infant rhesus monkeys wore spectacles with red filters or were raised in red light, they became consistently more hyperopic.[13,14] Similarly, light from red LEDs also acted as an inhibitory stimulus for axial eye growth in tree shrews, even in adolescent animals.[10,12] In contrast, upon their return to short-wavelength light, tree shrews tended to become more myopic.

Nonetheless, previous studies on the effect of various spectral compositions of light on refractive development have yielded inconsistent findings. In contrast to monkeys and tree shews, chickens,[24] guinea pigs[23] and fish[20] became more myopic under red light and more hyperopic under blue light, which was interpreted as an attempt by the eye to compensate for LCA. Why manipulations of the spectral composition have opposite effects in chicks, guinea pigs, and fish compared to tree shrews and rhesus monkeys is an important open question. The disparity of the results of previous studies highlights that our understanding of how chromatic cues influence eye growth is not complete. There are, however, similarities between the results of our study and previous studies in monkeys and tree shews, namely, that long-wavelength red light acted as an inhibitory stimulus for axial eye growth and induced hyperopic shift in children.

The choroid, a highly vascularized layer located between the retina and sclera, plays a crucial role in relaying signals derived from the retina to the sclera, producing mediators that regulate scleral metabolism during visual cue-modulated ocular development, further affecting extracellular matrix (ECM) remodelling in the sclera, and playing an active role in emmetropization or in the pathogenesis of myopia.[32,33] It has been determined that there is a direct correspondence between changes in choroid thickness and choroidal blood flow in both animal models and humans. Decreases in choroidal blood flow may result in reduced levels of oxygen and nutrient supply to the neighbouring avascular sclera.[33] Such modulation affects myopia development in experimental animal models and humans.[34,35] In this study, 650-nm red light therapy increased the choroidal thickness, possibly in response to an improvement in scleral blood perfusion through the choroid and reduced scleral hypoxia.

Previous studies have demonstrated that narrow-band, long-wavelength red light can thicken the choroid and restore the elasticity of scleral fibres.[33] When the choroid is exposed to 650-nm red light, the warm effect of the red light will open the neck-like stenosis at the opening of the small arteries of the choroidal lobules, increase the blood flow into the lobules, increase the microcirculation blood volume, increase the oxygen permeability of the choroidal blood vessels and the oxygen absorption capacity, and thicken the choroid. Additionally, the increase in choroid thickness can move the retina towards the focal plane of the eye (choroidal accommodation), change the AL.[32]

Various studies[36,37] on the association between the AL and choroidal thickness and the association between choroidal thickness and choroidal components in adults have been described with the help of binarization techniques applied to EDI-OCT images.[27,38,39] In myopic children, subfoveal choroidal thinning with longer ALs was found to be associated with a reduction in the LA.[28] Changes in the LA may directly influence choroidal thickness, as blood vessels represent the main component of the choroid, which might be a helpful signal for inhibiting myopia development.[28] Studies using chicks have shown that myopia resulted in smaller vessel diameters and lower blood vessel densities.[40,41] After short treatment durations (9 months), the SFChT, TCA and LA all significantly increased; however, the stromal area slightly decreased, with no significant difference compared to that at baseline. Univariate linear

regression analyses showed that the changes in the AL were significantly associated with age and baseline AL.

In conclusion, the results demonstrate that repeated 650-nm, low-intensity, single-wavelength red light effectively reduced myopia progression, inhibited axial elongation and increased the choroidal thickness, possibly in response to an improvement in scleral blood perfusion through the choroid and reduced scleral hypoxia. These findings require further exploration in a longitudinal study, as well as furth0er research in animal models.

Methods

Subjects

This study was a retrospective case series. Data from 106 subjects with myopia (aged 4 to 14 years; spherical equivalent refractive error [SER], -6.75 to -1.00 dioptres [D]) (Table 1) who sought vision correction between July 2019 and December 2019 at the Ningbo Eye Hospital and underwent eye examination that showed fast AL growth associated with rapid myopia progression were reviewed (Table 2). The study was approved by the Institutional Review Board of Ningbo Eye Hospital and carried out according to the tenets of the Declaration of Helsinki. Written informed consent was obtained from all patients.

Study Procedures

All the children wore spectacles and underwent repeated 650-nm, low-intensity, single-wavelength red light treatment twice a day for three minutes each time. Among the subjects, one child had anisometropia, and only the left eye was treated with red light because the right eye was emmetropic. We retrospectively reviewed patient medical records to extract the age, SER, AL, corneal curvature, treatment modality and follow-up data.

Researchers performed detailed ophthalmological examinations before treatment (baseline) and at each follow-up. Cycloplegic subjective refraction were conducted by experienced optometrists with three drops of 1% Tropicamide (Xing Qi Ophthalmic Co., Ltd, Shenyang, China) at five-minute intervals. The SER was calculated as the average of the spherical power and half the magnitude of the cylinder power. Ocular biometrics, including corneal curvature and AL were measured using a noncontact biometer (IOL Master; Carl Zeiss Meditec AG, Jena, Germany). Spectral domain optical coherence tomography (SD-OCT) was performed using a Heidelberg Spectralis instrument (Spectralis HRA + OCT, Heidelberg Engineering, Heidelberg, Germany), and the enhanced depth imaging (EDI) mode was used to enhance the visibility of the choroid. Subfoveal choroidal thickness (SFChT) was measured by two independent observers experienced in analysing OCT images using the Heidelberg linear measurement tool at the foveal location of the horizontal line scan. We defined the thinnest part of the macula in the image as the fovea. The SFChT was measured from the outermost part of the retinal pigment epithelium to the inner layer of the choroidoscleral interface.

Image Analysis

After recording the enhanced depth imaging optical coherence tomography (EDI-OCT) images, a high-quality image was displayed on a computer screen and independently evaluated by two trained examiners (QW and HC). When the two examiners determined that the choroidal image was eligible, the image was used for the following analyses. Binarization of the subfoveal choroidal area in the OCT image was done by a modified Niblack method. Briefly, the OCT image was analyzed by ImageJ (version 1.47; provided in the public domain by the National Institutes of Health, Bethesda, MD, USA; http://imagej.nih.gov/ij/).[25]

The examined area was selected to be 1500μm wide, with margins 750 μm nasal and 750 μm temporal to the fovea. It extended vertically from the RPE to the choroid–scleral interface, and the choroidal area was determined manually with the ImageJ ROI manager (Fig.1). Three choroidal vessels with lumens larger than 100 μm were randomly selected using the Oval Selection Tool on the ImageJ tool bar, and the average reflectivity of these areas was determined.[25-27] The average brightness of the luminal area was set as the minimum value to minimize the noise in the OCT image. The image was converted to 8 bits and adjusted using the Niblack Auto Local Threshold. Then the binarized image was converted to RGB image again, and the luminal area was determined using the Threshold Tool. After adjusting the Set Scale parameters by putting the pixel information of the acquired OCT image before the measurements, the total choroidal area (TCA), luminal area (LA), and of the stromal area were automatically calculated.[28] The light pixels were defined as the interstitial choroid or choroidal stroma, and the dark pixels were defined as the LA. The choroidal vascularity index (CVI) was defined as the ratio of LA to TCA.

Statistical Analyses

All statistical analyses were performed using SPSS version 23.0 (SPSS Inc., Chicago, IL, USA). All values were presented as the mean ± SD unless otherwise stated. Paired t-tests or Wilcoxon signed-rank tests were used to assess the differences between the baseline and the end follow-up visit for the SFChT, TCA, LA, stromal area and CVI. Changes in SER, AL, and corneal curvature between baseline and each follow-up visit in different subgroups were analysed by repeated-measures ANOVA. Associations of the demographic factors and ocular parameters were determined through univariate linear regression analyses. A P value < 0.05 was considered to be statistically significant.

Declarations

Disclosure

L. Zhou, None; W. Qiang, None; C. Hua, None; L. Tong, None

References

1. Holden, B. A. *et al.* Global Prevalence of Myopia and High Myopia and Temporal Trends from 2000 through 2050. *Ophthalmology* **123**, 1036-1042 (2016).

2. Morgan, I. G., Ohno-Matsui, K. & Saw, S. M. Myopia. *Lancet* **379**, 1739-1748 (2012).

3. Aller, T. A. Clinical management of progressive myopia. *Eye (Lond)* **28**, 147-153 (2014).

4. Lin, L. L., Shih, Y. F., Hsiao, C. K. & Chen, C. J. Prevalence of myopia in Taiwanese schoolchildren: 1983 to 2000. *Ann Acad Med Singap* **33**, 27-33 (2004).

5. You, Q. S. *et al.* Prevalence of myopia in school children in greater Beijing: the Beijing Childhood Eye Study. *Acta Ophthalmol* **92**, e398-406 (2014).

6. He, M. *et al.* Effect of Time Spent Outdoors at School on the Development of Myopia Among Children in China: A Randomized Clinical Trial. *JAMA* **314**, 1142-1148 (2015).

7. Scheiman, M. *et al.* Longitudinal changes in corneal curvature and its relationship to axial length in the Correction of Myopia Evaluation Trial (COMET) cohort. *J Optom* **9**, 13-21 (2016).

8. Mutti, D. O. *et al.* Corneal and crystalline lens dimensions before and after myopia onset. *Optom Vis Sci* **89**, 251-262 (2012).

9. Fang, P. C., Chung, M. Y., Yu, H. J. & Wu, P. C. Prevention of myopia onset with 0.025% atropine in premyopic children. *J Ocul Pharmacol Ther* **26**, 341-345 (2010).

10. Gawne, T. J., Ward, A. H. & Norton, T. T. Long-wavelength (red) light produces hyperopia in juvenile and adolescent tree shrews. *Vision Res* **140**, 55-65 (2017).

11. Shinhmar, H., Grewal, M., Sivaprasad, S., Hogg, C., Chong, V., Neveu, M. & Jeffery, G. Optically Improved Mitochondrial Function Redeems Aged Human Visual Decline. *J Gerontol A Biol Sci Med Sci* **75**, e49-49e52 (2020).

12. Gawne, T. J., Siegwart, J. T. Jr, Ward, A. H. & Norton, T. T. The wavelength composition and temporal modulation of ambient lighting strongly affect refractive development in young tree shrews. *Exp Eye Res* **155**, 75-84 (2017).

13. Smith, E. L. 3rd, Hung, L. F., Arumugam, B., Holden, B. A., Neitz, M. & Neitz, J. Effects of Long-Wavelength Lighting on Refractive Development in Infant Rhesus Monkeys. *Invest Ophthalmol Vis Sci* **56**, 6490-6500 (2015).

14. Hung, L. F., Arumugam, B., She, Z., Ostrin, L. & Smith, E. L. 3rd. Narrow-band, long-wavelength lighting promotes hyperopia and retards vision-induced myopia in infant rhesus monkeys. *Exp Eye Res* **176**, 147-160 (2018).

15. Liu, R. *et al.* The effects of monochromatic illumination on early eye development in rhesus monkeys. *Invest Ophthalmol Vis Sci* **55**, 1901-1909 (2014).

16. Xiong, F. *et al.* Orthokeratology and Low-Intensity Laser Therapy for Slowing the Progression of Myopia in Children. *Biomed Res Int* **2021**, 8915867 (2021).

17. Jones, L. A., Sinnott, L. T., Mutti, D. O., Mitchell, G. L., Moeschberger, M. L. & Zadnik, K. Parental history of myopia, sports and outdoor activities, and future myopia. *Invest Ophthalmol Vis Sci* **48**, 3524-3532 (2007).

18. Rose, K. A., Morgan, I. G., Ip, J., Kifley, A., Huynh, S., Smith, W. & Mitchell, P. Outdoor activity reduces the prevalence of myopia in children. *Ophthalmology* **115**, 1279-1285 (2008).

19. Foulds, W. S., Barathi, V. A. & Luu, C. D. Progressive myopia or hyperopia can be induced in chicks and reversed by manipulation of the chromaticity of ambient light. *Invest Ophthalmol Vis Sci* **54**, 8004-8012 (2013).

20. Kröger, R. H. & Fernald, R. D. Regulation of eye growth in the African cichlid fish Haplochromis burtoni. *Vision Res* **34**, 1807-1814 (1994).

21. Liu, R. *et al.* Effects of different monochromatic lights on refractive development and eye growth in guinea pigs. *Exp Eye Res* **92**, 447-453 (2011).

22. Ward, A. H., Norton, T. T., Huisingh, C. E. & Gawne, T. J. The hyperopic effect of narrow-band long-wavelength light in tree shrews increases non-linearly with duration. *Vision Res* **146-147**, 9-17 (2018).

23. Jiang, L. *et al.* Interactions of chromatic and lens-induced defocus during visual control of eye growth in guinea pigs (Cavia porcellus). *Vision Res* **94**, 24-32 (2014).

24. Wang, M., Schaeffel, F., Jiang, B. & Feldkaemper, M. Effects of Light of Different Spectral Composition on Refractive Development and Retinal Dopamine in Chicks. *Invest Ophthalmol Vis Sci* **59**, 4413-4424 (2018).

25. Sonoda, S., Sakamoto, T., Yamashita, T., Shirasawa, M., Uchino, E., Terasaki, H. & Tomita, M. Choroidal structure in normal eyes and after photodynamic therapy determined by binarization of optical coherence tomographic images. *Invest Ophthalmol Vis Sci* **55**, 3893-3899 (2014).

26. Agrawal, R., Gupta, P., Tan, K. A., Cheung, C. M., Wong, T. Y. & Cheng, C. Y. Choroidal vascularity index as a measure of vascular status of the choroid: Measurements in healthy eyes from a population-based study. *Sci Rep* **6**, 21090 (2016).

27. Sonoda, S. *et al.* Luminal and stromal areas of choroid determined by binarization method of optical coherence tomographic images. *Am J Ophthalmol* **159**, 1123-1131.e1 (2015).

28. Li, Z., Long, W., Hu, Y., Zhao, W., Zhang, W. & Yang, X. Features of the Choroidal Structures in Myopic Children Based on Image Binarization of Optical Coherence Tomography. *Invest Ophthalmol Vis Sci* **61**, 18 (2020).

29. Wu, P. C., Tsai, C. L., Wu, H. L., Yang, Y. H. & Kuo, H. K. Outdoor activity during class recess reduces myopia onset and progression in school children. *Ophthalmology* **120**, 1080-1085 (2013).

30. Zadnik, K. & Mutti, D. O. Outdoor Activity Protects Against Childhood Myopia-Let the Sun Shine In. *JAMA Pediatr* **173**, 415-416 (2019).

31. Rucker, F. J. The role of luminance and chromatic cues in emmetropisation. *Ophthalmic Physiol Opt* **33**, 196-214 (2013).

32. Wallman, J. *et al.* Moving the retina: choroidal modulation of refractive state. *Vision Res* **35**, 37-50 (1995).

33. Summers, J. A. The choroid as a sclera growth regulator. *Exp Eye Res* **114**, 120-127 (2013).

34. Chhablani, J. & Barteselli, G. Clinical applications of choroidal imaging technologies. *Indian J Ophthalmol* **63**, 384-390 (2015).

35. Zhang, S. *et al.* Changes in Choroidal Thickness and Choroidal Blood Perfusion in Guinea Pig Myopia. *Invest Ophthalmol Vis Sci* **60**, 3074-3083 (2019).

36. Ikuno, Y., Kawaguchi, K., Nouchi, T. & Yasuno, Y. Choroidal thickness in healthy Japanese subjects. *Invest Ophthalmol Vis Sci* **51**, 2173-2176 (2010).

37. El-Shazly, A. A., Farweez, Y. A., ElSebaay, M. E. & El-Zawahry, W. Correlation between choroidal thickness and degree of myopia assessed with enhanced depth imaging optical coherence tomography. *Eur J Ophthalmol* **27**, 577-584 (2017).

38. Alshareef, R. A., Khuthaila, M. K., Goud, A., Vupparaboina, K. K., Jana, S. & Chhablani, J. Subfoveal Choroidal Vascularity in Myopia: Evidence From Spectral-Domain Optical Coherence Tomography. *Ophthalmic Surg Lasers Imaging Retina* **48**, 202-207 (2017).

39. Gupta, P. *et al.* Characterization of Choroidal Morphologic and Vascular Features in Young Men With High Myopia Using Spectral-Domain Optical Coherence Tomography. *Am J Ophthalmol* **177**, 27-33 (2017).

40. Hirata, A. & Negi, A. Morphological changes of choriocapillaris in experimentally induced chick myopia. *Graefes Arch Clin Exp Ophthalmol* **236**, 132-137 (1998).

41. Junghans, B. M., Crewther, S. G., Liang, H. & Crewther, D. P. A role for choroidal lymphatics during recovery from form deprivation myopia. *Optom Vis Sci* **76**, 796-803 (1999).
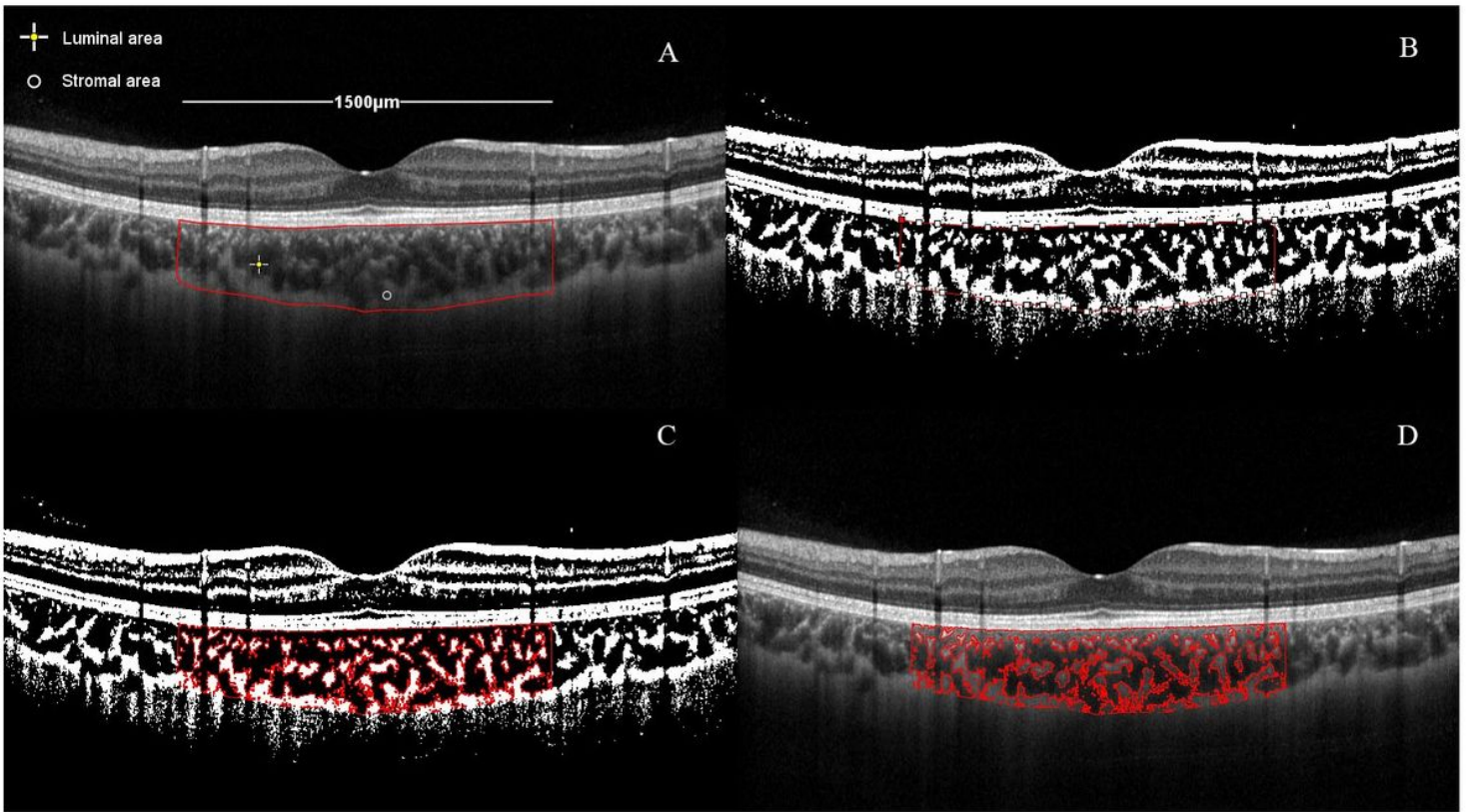
Figures

Figure 1

Binarization analysis of choroidal structure from OCT images. (A) Determination of 1.5mm segmentation block of the subfoveal choroidal area in the original EDI-OCT image with the ImageJ ROI manager. The luminal area (dark area, cross) and the stromal area (circle) are seen. (B) Identification of the choroidal segments using the binarization technique. (C) The rectangle surrounded by a red line was excised, and the dark areas were traced by the Niblack method. (D) Overlay of the target choroidal region created by image binarization on the EDI-OCT image.
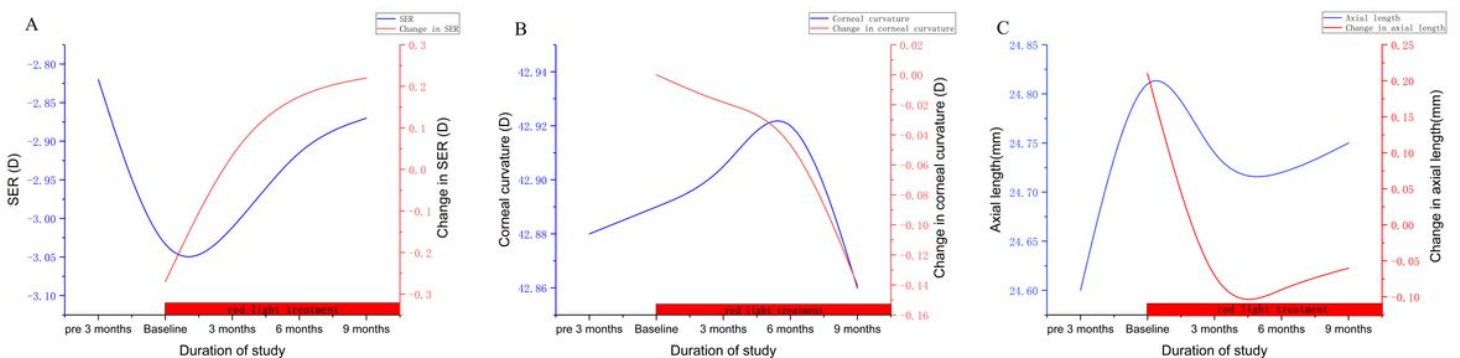

Figure 2

Changes in the biometric measurements of the treated eyes are shown. There was an increase in spherical equivalent refractive error (SER) (A), corneal curvature (CC) (B) and axial length (AL) (C) before red light therapy, and the trend was opposite after treatment except the corneal curvature.
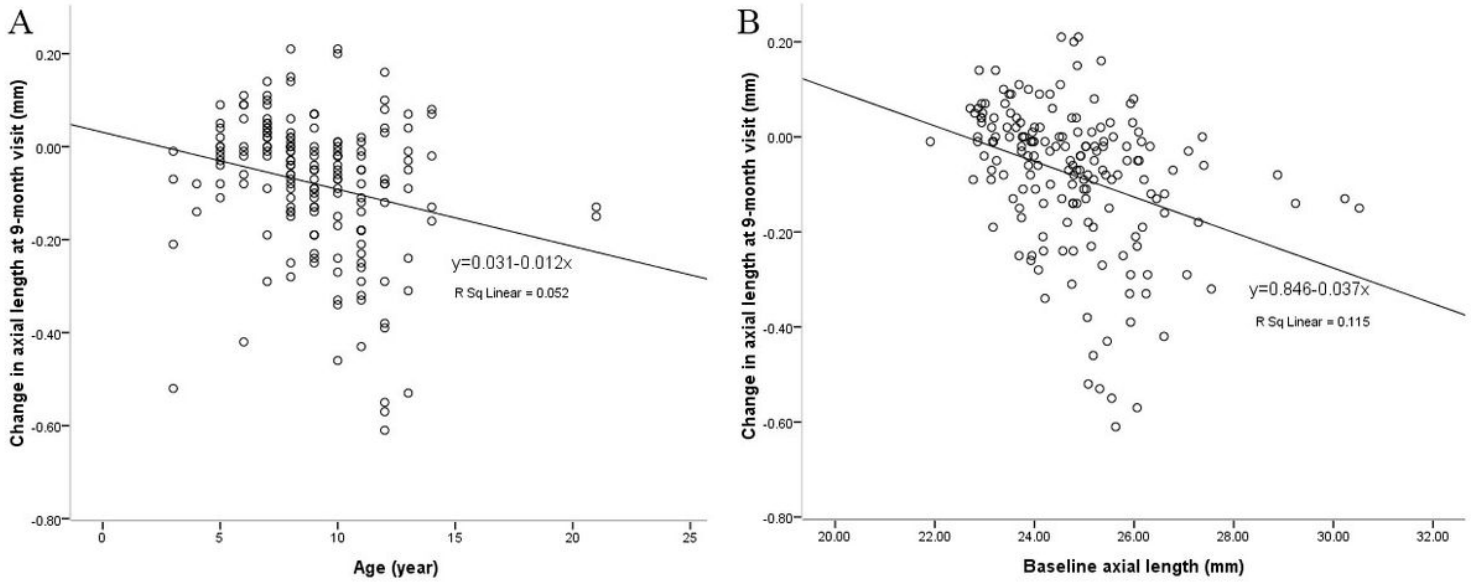
Figure 3

Relationship between the changes in axial length and the baseline factors determined through univariate analyses. (A) The change in axial length showed a borderline association with age (R = -0.229, P = 0.002). (B) Baseline axial length was significantly associated with the change in axial length (R = -0.34, P⬚0.001).